Scientific Inquiry and Review (SIR)
Volume 8 Issue 1, 2024
ISSN $_{(P)}$: 2521-2427, ISSN $_{(E)}$: 2521-2435
Homepage: https://journals.umt.edu.pk/index.php/SIR

Article QR

Title:	**Impact of Basic Bath on Optical and Electrical Characteristics of Zinc Sulfide (ZnS) Thin Films**
Author (s):	Muhammad Tahir[1], Zaheer Hussain Shah[1], Muhammad Imran[2], Bilal Ramzan[1], Saira Riaz[3] and Shahzad Naseem[3]
Affiliation (s):	[1] University of Management and Technology, Lahore, Pakistan [2] University of Educatiuon, Lahore, Pakistan [3]Centre of Excellence in Solid State Physics, University of the Punjab, Lahore, Pakistan
DOI:	https://doi.org/10.32350/sir.81.05
History:	Received: July 19, 2023, Revised: November 29, 2023, Accepted: November 30, 2023, Published: March 15, 2024
Citation:	Imran M,Tahir M, Shah ZH, Ramzan B, Riaz S, Naseem S. Impact of Basic Bath on Optical and Electrical Characteristics of Zinc Sulfide (ZnS) Thin Films. *Sci Inq Rev.* 2024;8(1):75–93. https://doi.org/10.32350/sir.81.05
Copyright:	© The Authors
Licensing:	This article is open access and is distributed under the terms of Creative Commons Attribution 4.0 International License
Conflict of Interest:	Author(s) declared no conflict of interest

A publication of
The School of Science
University of Management and Technology, Lahore, Pakistan

Impact of Basic Bath on Optical and Electrical Characteristics of Zinc Sulfide (ZnS) Thin Films

Muhammad Tahir[1*], Zaheer Hussain Shah[1], Muhammad Imran[2], Bilal Ramzan[1], Saira Riaz[3] and Shahzad Naseem[3]

[1]University of Management and Technology, Lahore, Pakistan
[2]University of Education, Lahore, Pakistan
[3]Centre of Excellence in Solid State Physics, University of the Punjab, Lahore, Pakistan

ABSTRACT

Zinc Sulfide (ZnS) thin films have attracted the research community because of their recognition in optoelectronic devices. An electroless, application-oriented, CBD (chemical bath deposition) method is typically applied for the deposition of ZnS thin films deposited on a glass substrate with pH 8. Deposition temperature is varied as 25℃, 50℃, 75℃, 100℃, and 125℃. In this study, ZnS thin films and X-ray diffraction (XRD) Variable Angle Spectroscopic Ellipsometry was used. XRD analysis confirmed the hexagonal structure of deposited ZnS thin films at all temperatures. Ellipsometric results showed high transmission (∼ 65%) in the visible region for thin films prepared with 50°C deposition temperature and high refractive index at wavelength (λ = 550nm) ∼2.04. Variation in the direct band gap (E_g), 3.86–3.99 eV, was studied for synthesized thin films of ZnS. Improvement in optimizing the optical properties of ZnS thin films indicated an effective optoelectronic application.

Keywords: chemical bath deposition, direct bandgap, high transmission, optoelectronics

Highlights

- ZnS has potential applications in optoelectronic devices.
- No complex agents were used.
- High transmission was recorded.

1. INTRODUCTION

In comparison to bulk structured materials, nanostructures have recently emerged as a possible alternative. Regardless of their size, they induce a vast amount of potential applications for device fabrications which can be

* Corresponding Author: muhammad.tahir@umt.edu.pk

fruitful for everyday use [1, 2]. Thin films have distinguished themselves from other nanostructures over the years due to their remarkable properties. All optoelectronic devices can be employed by using thin films because of their optical and electrical properties [3, 4]. A valuable wide bandgap semiconductor that attracts the attention of the semiconductor industry is zinc sulfide (ZnS). ZnS belongs to an important family of semiconductors (II-IV) offering a 3.7 eV energy gap and a large absorption coefficient which is suitable for fabricating anti-reflection coatings [5–7].

ZnS thin films are a highly favorable candidate for applications in optoelectronic devices, for example, electroluminescent devices and photovoltaic (PV) cells [8]. This is because of their promising attributes towards wide range bandgap and n-type conductivity. These properties enable the transmission of highly energetic photons reaching to junction, thus improving the reaction of blue response in PV cells [9]. Moreover, ZnS thin film is a well-known semiconducting material for potential applications in light-emitting diodes that operate well in the blue region owing to its huge direct energy band gap. Most of the reports available regarding the energy bandgap properties of ZnS films demonstrate that in its cubic form along with lattice constant, a=0.541nm; c=2.49nm, it exhibits a direct energy gap of 3.68eV at 295K. Conversely, in the case of a hexagonal with a direct energy band gap between 3.74 and 3.87 eV at 300 K with a lattice constant of a = 0.382 nm and c = 2.49 nm. The optical properties of ZnS films including their n (refractive index) and k (extinction coefficient) values have been calculated and studied [10].

Over the last decade, several studies reported on the fabrication of ZnS films by chemical and physical techniques [11–13]. Several methods including thermal evaporation, sputtering, sol-gel, and CBD (chemical bath deposition) have all been investigated to synthesize ZnS thin films [14–17]. The CBD method is a well-known deposition technique that stands out among all others due to its cost-effectiveness, providing a non-vacuum atmosphere and allowing large-area deposition. This technique is particularly suitable as it doesn't involve the use of any advanced instruments. Moreover, CBD offers the flexibility of using a variety of substrates that can be utilized in the deposition process at low temperatures. Low-temperature deposition procedure not only reduces the layer of oxides on the substrates but also helps to prevent the film from substrate corrosion [18].

In the current work, a chemical method that included the CBD technique was employed to fabricate ZnS thin films. This research aims to study the necessary conditions to deposit high-quality ZnS thin films from CBD. Moreover, it intends to calculate their optical properties including transmission, refractive index, energy bandgap, and extinction coefficient. Furthermore, it strives to optimize the conditions of the deposition technique for ZnS thin films.

2. SYNTHESIS DETAILS

The most advantageous method for developing thin films on a variety of surfaces is CBD. This method is mostly utilized for the synthesis of thin films, such as zinc sulfide, zinc oxide, zinc selenide, and lead sulfide because of its amazing benefits and low cost of production. CBD also synthesizes ternary composite [19]. In this study, this method was utilized for the synthesis of ZnS thin films. Zinc acetate and thiourea were taken as precursors. Zn^{2+} ion from zinc acetate while S^{2-} from thiourea were used. Zinc acetate was mixed in DI water under continuous stirring at room temperature. Similarly, thiourea was mixed in DI water under continuous stirring to form a homogeneous solution. Both solutions were mixed under continuous stirring for 2 hours. Ammonia was added dropwise to adjust the pH of the solution. Properly cleaned glass slides were adjusted in the holder and dipped in the beaker for the deposition of ZnS thin films. A series of these thin films was deposited by varying bath temperature from 25°C to 125°C for 1 hour. These thin films were dried at room temperature. The synthesis detail is shown in Figure 1.

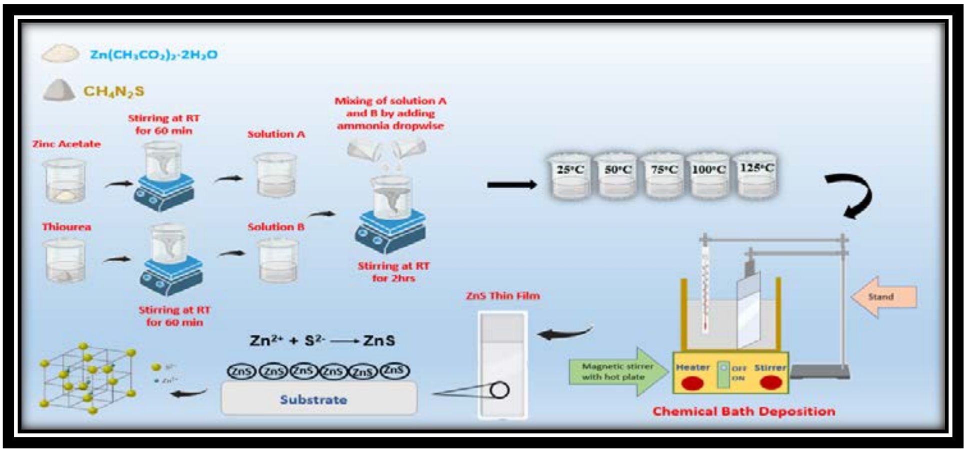

Figure 1. Synthesis Detail of ZnS Thin Films by Varying Bath Temperature

3. RESULTS AND DISCUSSION

Figure 2 (a-e) depicts the XRD pattern of the prepared ZnS thin films with varying temperatures via CBD. All the planes (1014), (100), (103), (1010), (104), (1011), (2013), (2014) of ZnS thin films clearly indicate the formation of hexagonal phase matched with JCPDS card no 01-072-0162 under all conditions.

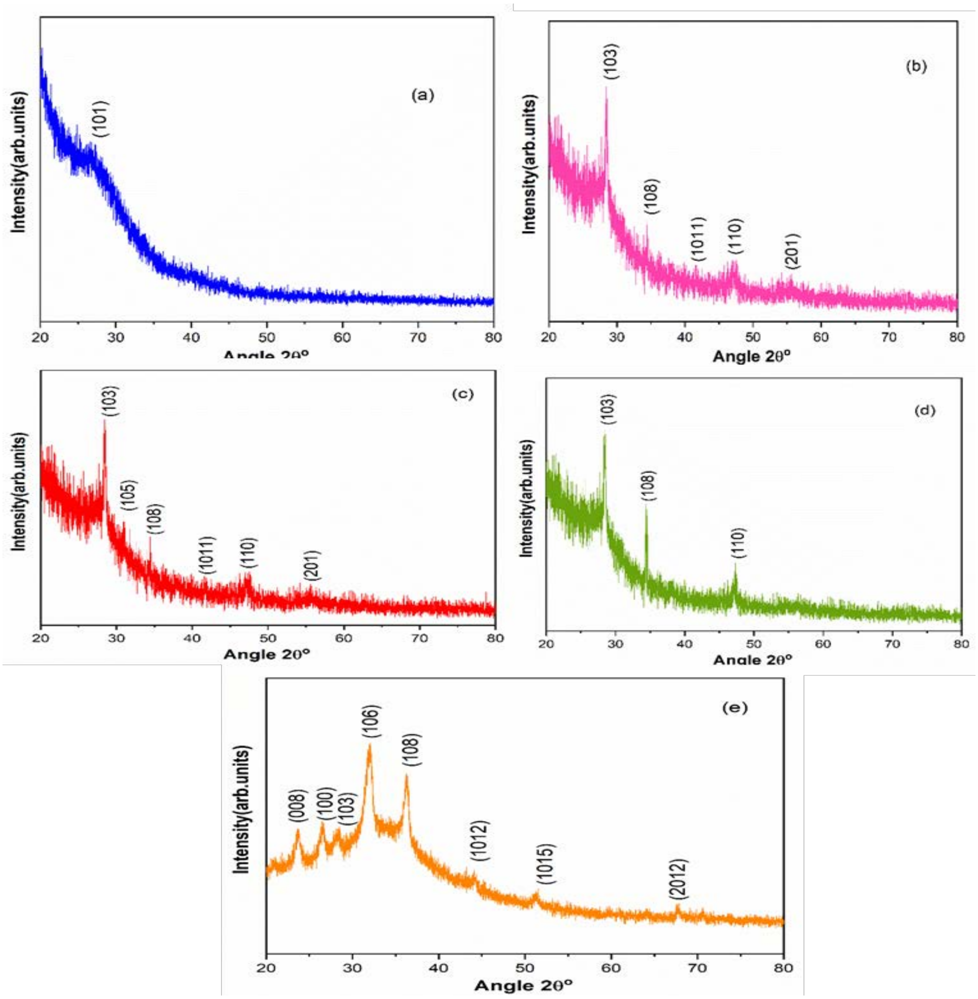

Figure 2. XRD Patterns of ZnS thin Films at Bath Temperatures (a) 25℃(b) 50℃ (c) 75℃ (d)100℃ (e)125℃

For the analysis of several parameters, such as crystal growth, phase orientation, and the type of phase of thin films XRD was utilized. For the determination of crystallite size, dislocation density, and strain, Scherer formula [20] was used which is shown below in equation 1,

$$D= k\lambda/\beta\cos\theta \quad (1)$$

where D is the average of nano-crystallite size [21], k depicts shape factor (0.90), λ represents wavelength radiation (0.15406nm) of Cu Kα [22], β shows full width at half maximum (FWHM) [23], and θ is the Bragg's angle of the most preferred orientation plane [24].

Dislocation density is the inverse of crystallite size and it is calculated by the formula given below in equation 2 [25],

$$\delta= 1/D^2 \quad (2)$$

Strain is calculated by using the formula [26] given below in equation 3,

$$\text{Strain} = \beta/(4\tan\theta) \quad (3)$$

Parameters calculated from eqs 1-3 are given below in Table 1.

Table 1. Parameters Calculated from XRD of ZnS thin Films

Sample	Crystallite size D(nm)	Dislocation Density (δ)	Strain
A	Amorphous	Amorphous	Amorphous
B	32.77	0.0009312	0.004301
C	29.25	0.0011681	0.004819
D	27.30	0.0013409	0.005162
E	19.66	0.0025855	0.006404

The use of ZnS in optoelectronics devices and many other applications requires high transparency of light in the visible region of wavelength 400-800nm [27]. The transmittance spectra of series samples a,b,c,d, and e against wavelength are shown in Figure 3.

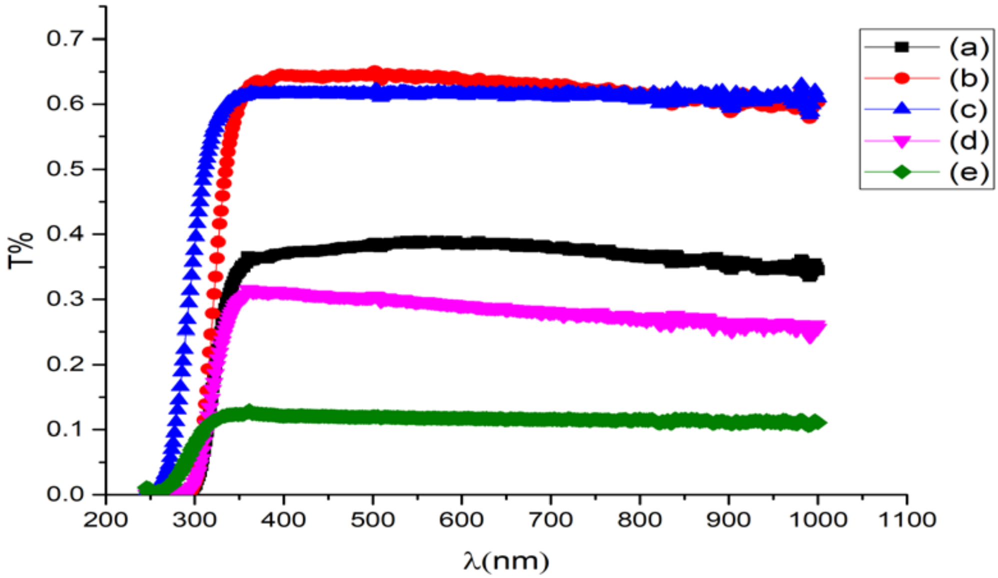

Figure 3. Transmission Spectra of ZnS Thin Films with Varying Temperature

In the region of transparency, the value of transmittance can be found by using the free carrier of absorption. The value of transmission increased with temperature increase. The difference between sample ‘b’ and sample ‘a’ was studied. The transmission values of 36%, 65%, 62%, 32%, and 14% were observed at varying deposition temperatures, that is, 25℃, 50℃, 75℃, 100℃, and 125℃ given in Table 2.

Table 2. Percentage Transmission of ZnS Thin Films

Samples	Conditions	Transmission
A	ZnS thin film at temperature 25℃ with stirring 1hr	36%
B	ZnS thin film at temperature 50℃ with stirring 1hrs	65%
C	ZnS thin film at temperature 75℃ with stirring 1hr	62%
D	ZnS thin film at temperature 100℃ with stirring 1hrs	32%
E	ZnS thin film at temperature 125℃ with stirring 1hr	14%

In optical applications, energy band gaps are very important. The series of sample ZnS thin films synthesized by the CBD method had their energy band gap measured from the information data collected by spectroscopic ellipsometry [28]. Tauc's relation was utilized to calculate the optical band gap for each sample at various conditions. Absorption coefficient (α) with the optical band gap was calculated using the relation in equation 4 [29] given below,

$$\alpha = \left(\frac{k}{h\nu}\right)(h\nu - Eg)^{n} \quad (4)$$

where k represents constant, h represents Planck's constant [30], hν shows photon energy, E_g is band energy, and n are numbers that illustrate the nature of electron transition between the valance band and conduction band. If n = 2, it represents the semiconductor direct band gap.

To calculate band energy, $(\alpha)^2$ against photon energy was plotted as linear to absorption coefficient that reported a direct band gap transition of the prepared material. Tauc's plots [31] were used to calculate band energy and its nature for all samples represented in Table 3.

Figure 4 confirmed the energy band gap of ZnS thin films at varying temperatures. The observed band gap varies from 3.86-3.99eV. The maximum band gap of 3.99eV was observed at 100℃.

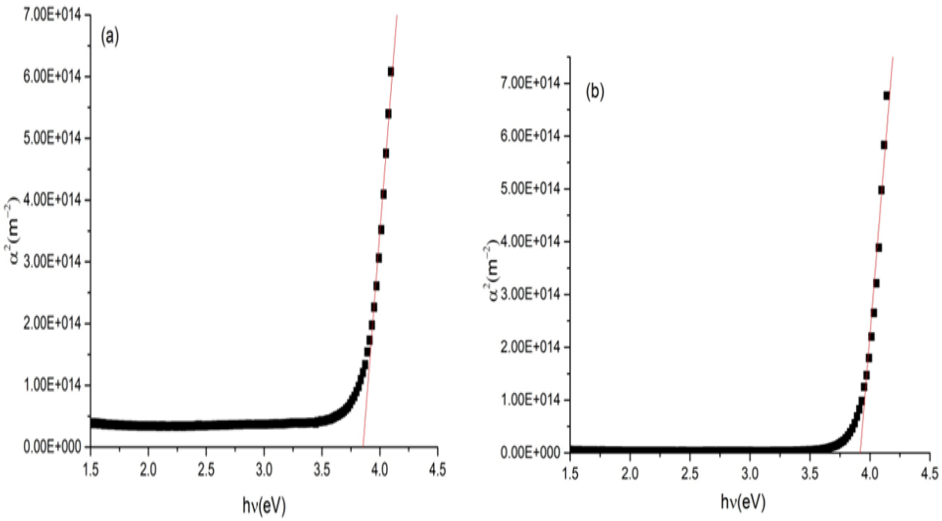

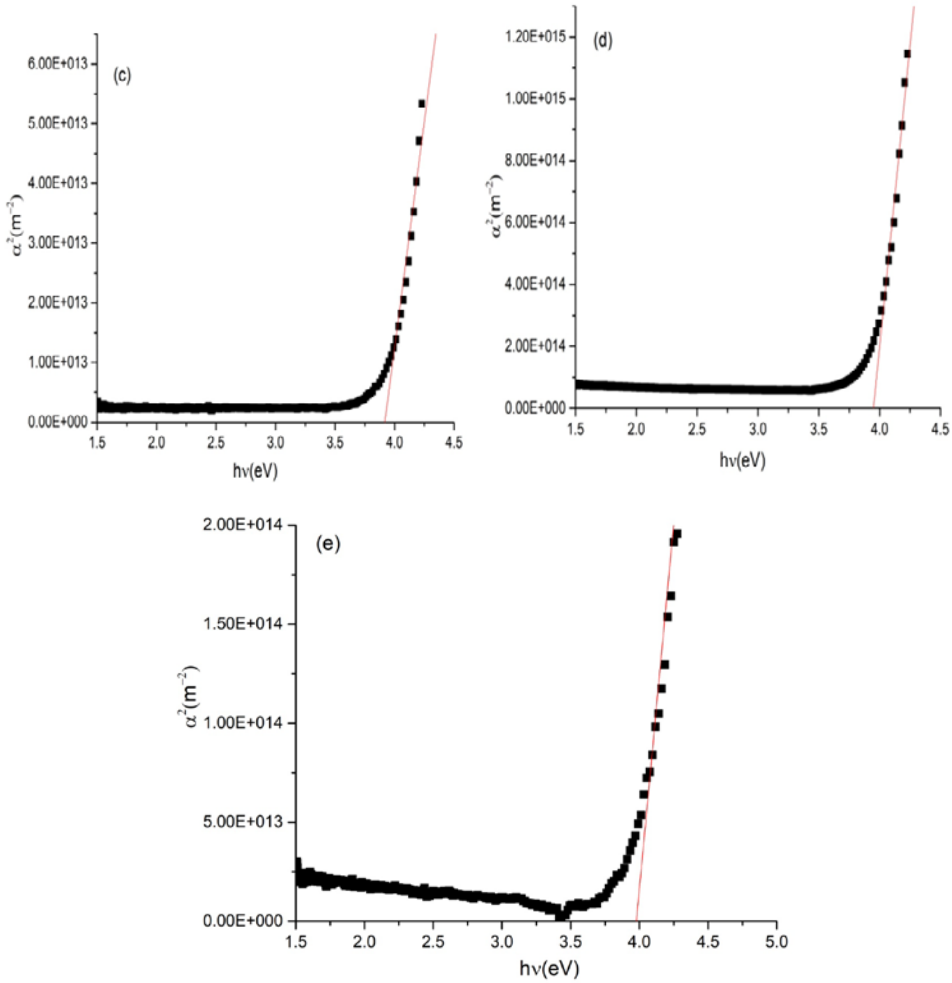

Figure 4. Band Gap of ZnS Thin Films with Varying Deposition Temperature (a) 25℃ (b) 50℃ (c)75℃ (d)100℃ and (e)125℃

Table 3. Energy Band Gap of ZnS Thin Films

Sample	Deposition Time	Temperature (℃)	E_g(eV)
A	1hr	25	3.86
B	1hr	50	3.91
C	1hr	75	3.93
D	1hr	100	3.97
E	1hr	125	3.99

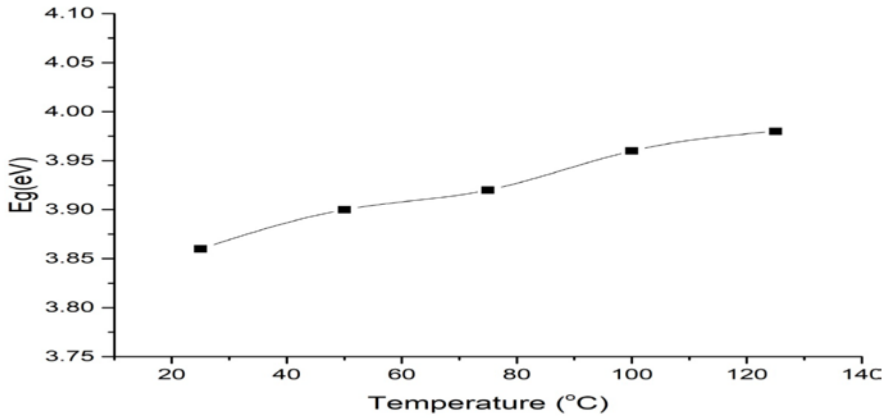

Figure 5. Variation in Band Gap with Temperature

The variations in refractive index with wavelength at all conditions are presented in Figure 5. Notably, with the addition of ammonia, the value of the refractive index increases [32]. To calculate optical quantities in the visible region and UV region, Cauchy's relation was used. Cauchy's equation is given below in equation 5 [33].

$$n(\lambda) = A + \frac{B}{\lambda 2} + \frac{C}{\lambda 2} \quad (5)$$

In this equation, A, B, and C are represented as constants.

The extinction coefficient is an important optical parameter [34]. It measures the materials that absorb light with a given wavelength [35]. It has a direct relation to the absorption of light. The extinction coefficient varies with the transmission of light. If transmission has a greater value, then k values are smaller. This shows that the material with a small k value has high transparency [36].

Refractive index and extinction coefficient against the wavelength of sample "a" is depicted below in Figure 6. The sample was synthesized at a temperature of 25°C. The refractive index was observed at 2.19 and the extinction coefficient was observed at 0.008. To observe the refractive index (n) and extinction coefficient (k) for sample "b", the sample was prepared at a temperature of 50°C. The refractive index value was 2.12 for sample "b", whereas the extinction coefficient value was 0.066. Similarly, sample "c" was prepared at a temperature of 75°C. The refractive index value was 1.62 and the extinction coefficient value was observed as 0.055. It shows that with temperature increases, refractive index value also increases. Sample “d” was prepared at a temperature of 100℃. The refractive index value and extinction coefficient value were observed. The value of refractive index was 2.16 and that of extinction coefficient was 0.06. Similarly, sample “e” was prepared at a temperature of 125℃, as shown in Table 4. The value of the refractive index was observed as 2.14 and the value of the extinction coefficient was observed as 0.073. This shows that the sample has a small value of refractive index and extinction coefficient.

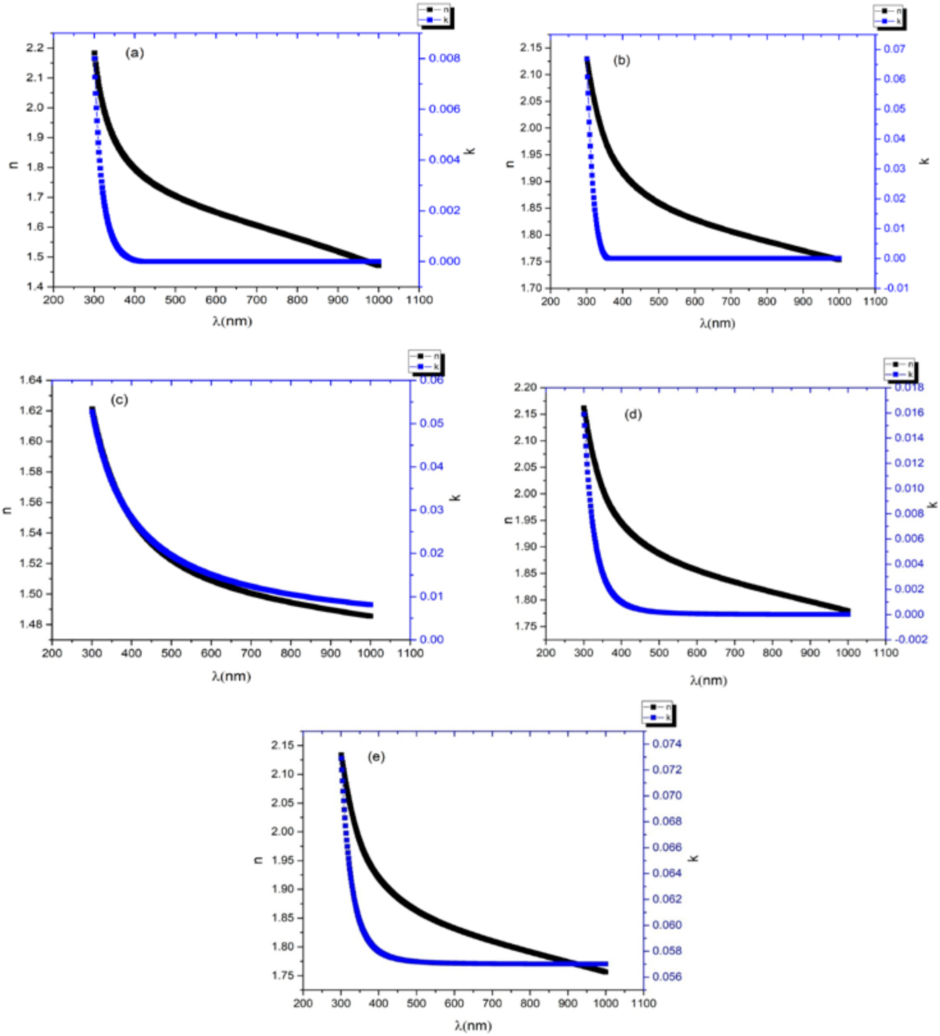

Figure 6. n and k of ZnS Thin films with Varying Deposition Temperature (a) 25℃(b) 50℃ (c)75℃ (d)100℃ (e)125℃

Table 4. n and k for All Samples

Sample	Condition	Deposition Time	n(400nm)	K
A	Temperature 25°C	1hr	2.2	0.008
B	Temperature 50°C	1hr	2.12	0.066
C	Temperature 75°C	1hr	1.62	0.055
D	Temperature 100°C	1hr	2.16	0.016
E	Temperature 125°C	1hr	2.14	0.073

The dielectric constant of ZnS thin films synthesized at various temperatures was calculated using the equations 6 [37] and 7 [38] given below.

$$\varepsilon_1 = n^2 - k^2 \tag{6}$$

$$\varepsilon_2 = 2nk \tag{7}$$

Where ε_1 shows the real part of dielectrics and ε_2 shows the imaginary part of the optical dielectric constant for ZnS thin films.

Figure 7 shows the real and imaginary parts of thin films of the dielectric constant on the wavelength. The plot shows that with temperature increases the values of the optical dielectric constant decrease. Dielectric constants are listed in Table 5.

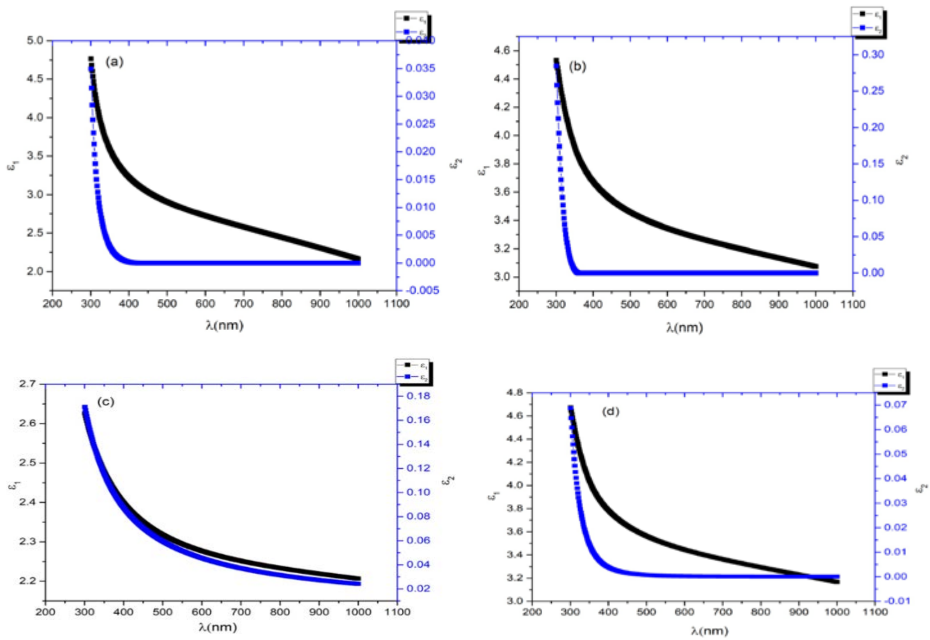

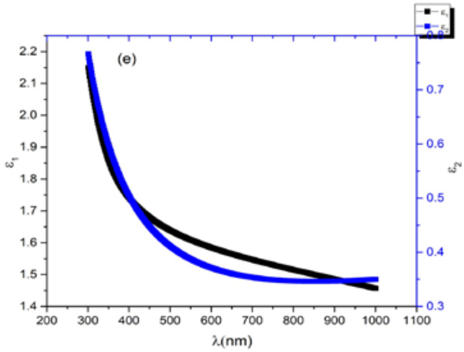

Figure 7. ε_1 & ε_2 of ZnS Thin Films with Varying Deposition Temperature (a) 25℃ (b) 50℃ (c) 75℃ (d) 100℃ (e) 125℃

Table 5. Optical Dielectric Constant of Samples

Sample	Conditions	ε1	ε2
A	Temperature 25°C	4.8	0.035
B	Temperature 50°C	4.52	0.27
C	Temperature 75°C	2.63	0.17
D	Temperature 100°C	4.65	0.07
E	Temperature 125°C	2.15	0.78

The measured electrical properties included resistivity and conductivity. The resistivity of ZnS thin films was measured via the Hall effect [39] and the Van der Pauw method [40]. In this method, there are four probes; a current of 1mA is applied through the 1 and 3 probe and voltage is calculated with the 2 and 4 probe [41]. The applied magnetic field and the applied voltage are 1T and 0.9V, respectively [42]. Voltage is measured in the presence and absence of a magnetic field, respectively. Thus, if the applied voltage sign is positive, then only a single sample is A n-type and all the remaining samples comprise p-type carriers [43]. Resistivity and conductivity are calculated by using the equations [44–46],

$$R = V/I \tag{8}$$

$$\rho = RA/l \tag{9}$$

$$\sigma = 1/\rho \tag{10}$$

where R is resistance, ρ is resistivity, and σ is the conductivity of the sample [47]. For the ZnS thin films, resistivity and conductivity are depicted in

Figure 8. The figure shows that by increasing bath temperature resistivity of the ZnS thin films, resistance increases and conductivity decreases.

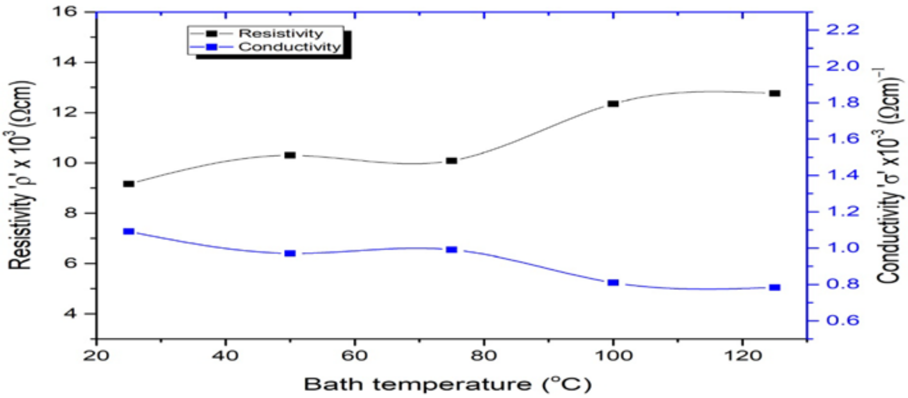

Figure 8. ρ & σ of ZnS Thin Films Varying Deposition Temperature (a) 25℃ (b) 50℃ (c) 75℃ (d) 100℃ (e) 125℃

4. CONCLUSION

ZnS (zinc sulfide) is among the most significant II-VI semiconductor materials due to its distinct optical properties. An electroless, CBD technique was used for the synthesis of ZnS thin films. The films were deposited on the glass substrates. The deposition temperature was varied as 25℃, 50℃, 75℃, 100℃, and 125℃. ZnS thin films were utilised by employing XRD (X-ray Diffractometer) and spectroscopic ellipsometry. XRD analysis confirmed the hexagonal structure of these thin films. Ellipsometry results showed high transmission (~65%) in the visible part of the electromagnetic spectrum for thin films prepared with 50℃ deposition temperature and high refractive index (at λ =550nm) ~2.04. Diversity in the direct band gap 3.86–3.99 eV was also observed for the prepared thin films. The study concludes that the enhanced optical characteristics of ZnS thin films are appropriate for effective optoelectronic applications.

CONFLICT OF INTEREST

The authors of the manuscript have no financial or non-financial conflict of interest in the subject matter or materials discussed in this manuscript.

DATA AVAILABILITY STATEMENT

All relevant data has been used in the manuscript.

REFERENCES

1. Li P, Chen S, Dai H, et al. Recent advances in focused ion beam nanofabrication for nanostructures and devices: Fundamentals and applications. *Nanoscale*. 2021;13(3):1529–1565. https://doi.org/10.1039/D0NR07539F
2. Shen G, Chen D. One-dimensional nanostructures and devices of II–V group semiconductors. *Nanoscale Res Lett*. 2009;4(8):779–788. https://doi.org/10.1007/s11671-009-9338-2
3. Chopra K. *Thin Film Device Applications*. Springer Science & Business Media; 2012.
4. Strukov DB, Kohlstedt H. Resistive switching phenomena in thin films: Materials, devices, and applications. *MRS Bull*. 2012;37(2):108–114. https://doi.org/10.1557/mrs.2012.2
5. Abel S, Tesfaye JL, Kiran R, et al. Studying the effect of metallic precursor concentration on the structural, optical, and morphological properties of zinc sulfide thin films in photovoltaic cell applications. *Adv Mater Sci Eng*. 2021;2021:1–6. https://doi.org/10.1155/2021/7443664
6. Bashar MS, Matin R, Sultana M, et al. Effect of rapid thermal annealing on structural and optical properties of ZnS thin films fabricated by RF magnetron sputtering technique. *J Theor Appl Phys*. 2020;14:53–63. https://doi.org/10.1007/s40094-019-00361-5
7. Barman B, Bangera KV, Shivakumar GK. Preparation of thermally deposited Cux(ZnS)1-x thin films for opto-electronic devices. *J Alloys Compd*. 2019;772:532–536. https://doi.org/10.1016/j.jallcom.2018.09.192
8. Goktas A, Tumbul A, Aba Z, Kilic A, Aslan F. Enhancing crystalline/optical quality, and photoluminescence properties of the Na and Sn substituted ZnS thin films for optoelectronic and solar cell applications; a comparative study. *Opt Mater*. 2020;107:e110073. https://doi.org/10.1016/j.optmat.2020.110073
9. Göde F, Gümüş C, Zor M. Investigations on the physical properties of the polycrystalline ZnS thin films deposited by the chemical bath deposition method. *J Cryst Growth*. 2007;299(1):136–141. https://doi.org/10.1016/j.jcrysgro.2006.10.266

10. Arenas OL, Nair MTS, Nair PK. Chemical bath deposition of ZnS thin films and modification by air annealing. *Semicond Sci Technol*. 1997;12(10):e1323. https://doi.org/10.1088/0268-1242/12/10/022
11. Shah ZH, Ahmad I, Tahir QA, Khawaja EE. On the determination of refractive index and thickness of thin dielectric films from measurement of transmittance. *Surf Rev Lett*. 2012;19(06):e1250059. https://doi.org/10.1142/S0218625X1250059X
12. Zeng X, Pramana SS, Batabyal SK, et al. Low-temperature synthesis of wurtzite zinc sulfide (ZnS) thin films by chemical spray pyrolysis. *Phys Chem Chem Phys*. 2013;15(18):6763–6768. https://doi.org/10.1039/C3CP43470B
13. Ghasemi H, Mozaffari MH, Moradian R. Effects of deposition time on structural and optical properties of ZnS and ZnS/Au thin films grown by thermal evaporation. *Phy B: Condens Matter*. 2022;627:e413616. https://doi.org/10.1016/j.physb.2021.413616
14. Priya K, Ashith VK, Rao GK, Sanjeev G. A comparative study of structural, optical, and electrical properties of ZnS thin films obtained by thermal evaporation and SILAR techniques. *Ceram Int*. 2017;43(13):10487–10493. https://doi.org/10.1016/j.ceramint.2017.05.094
15. Pathak TK, Kumar V, Purohit LP, Swart HC, Kroon RE. Substrate-dependent structural, optical, and electrical properties of ZnS thin films grown by RF sputtering. *Physica E: Low-dimen Sys Nanost*. 2016;84:530–536. https://doi.org/10.1016/j.physe.2016.06.020
16. Li X, Zhu X, Jin K. Study on structural and optical properties of Mn-doped ZnO thin films by sol-gel method. *Opt Mater*. 2020;100:e109657. https://doi.org/10.1016/j.optmat.2020.109657
17. Arandhara G, Bora J, Saikia PK. Effect of pH on the crystallite size, elastic properties, and morphology of nanostructured ZnS thin films prepared by chemical bath deposition technique. *Mater Chem Phys*. 2020;241:e122277. https://doi.org/10.1016/j.matchemphys.2019.122277
18. Pawar SM, Pawar BS, Kim JH, Joo OS, Lokhande CD. The recent status of the chemical bath deposited metal chalcogenide and metal oxide thin films. *Curr Appl Phys*. 2011;11(2):117–161. https://doi.org/10.1016/j.cap.2010.07.007

19. Seshan K. *Handbook of Thin Film Deposition Techniques: Principles, Methods, Equipment and Applications*. 2nd ed. CRC Press; 2002.
20. Heavens OS. *Optical Properties of Thin Solid Films*. Courier Corporation; 1991.
21. Blois MS Jr. Preparation of thin magnetic films and their properties. *J Appl Phys*. 1955;26(8):975–980. https://doi.org/10.1063/1.1722148
22. Tang ZX, Yu Z, Zhang ZL, Zhang XY, Pan QQ, Shi LE. Sonication-assisted preparation of CaO nanoparticles for antibacterial agents. *Quim Nova*. 2013;36(7):933–936. https://doi.org/10.1590/S0100-40422013000700002
23. Mirghiasi Z, Bakhtiari F, Darezereshki E, Esmaeilzadeh E. Preparation and characterization of CaO nanoparticles from Ca(OH)2 by direct thermal decomposition method. *J Ind Eng Chem*. 2014;20(1):113–117. https://doi.org/10.1016/j.jiec.2013.04.018
24. Zelati A, Amirabadizadeh A, Kompany A. Preparation and characterization of barium carbonate nanoparticles. *Int J Chem Eng Appl*. 2011;2(4):299–303. https://doi.org/10.7763/IJCEA.2011.V2.121
25. Wei A, Liu J, Zhuang M, Zhao Y. Preparation and characterization of ZnS thin films prepared by chemical bath deposition. *Mater Sci Semicond Proc*. 2013;16(6):1478–1484. https://doi.org/10.1016/j.mssp.2013.03.016
26. Priya K, Rao GK, Sanjeev G. The fabrication and characterization of thermal evaporated n-ZnS/p-Si heterojunction and ZnS-Au Schottky photodiodes. *Opt Laser Technol*. 2023;157:e108657. https://doi.org/10.1016/j.optlastec.2022.108657
27. Padmavathy V, Sankar S, Ponnuswamy V. Influence of thiourea on the synthesis and characterization of chemically deposited nano-structured zinc sulfide thin films. *J Mater Sci: Mater Electron*. 2018;29(9):7739–7749. https://doi.org/10.1007/s10854-018-8770-4
28. Wang X, Yu C, Wu J, Wei Z, Zhang Y. Solvothermal synthesis of superhydrophobic ZnS film. *Asian J Chem*. 2013;25(3):e1241.
29. Mousavi SM, Kafashan H. Physical properties of Cd-doped ZnS thin films. *Superlatt Microst*. 2019;126:139–149. https://doi.org/10.1016/j.spmi.2018.12.002

30. Cheng Y, Li W, Fan X, Liu J, Xu W, Yan C. Modified multi-walled carbon nanotube/Ag nanoparticle composite catalyst for the oxygen reduction reaction in an alkaline solution. *Electro Acta*. 2013;111:635–641. https://doi.org/10.1016/j.electacta.2013.08.034
31. Eryong N, Donglai L, Yunsen Z, et al. Photoluminescence and magnetic properties of Fe-doped ZnS nanoparticles synthesized by chemical co-precipitation. *Appl Surf Sci*. 2011;257(21):8762–8766. https://doi.org/10.1016/j.apsusc.2011.03.114
32. Yoo D, Choi MS, Chung C, Heo SC, Choi C. Characteristics of radio frequency-sputtered ZnS on the flexible polyethylene terephthalate (PET) substrate. *J Nanosci Nanotechnol*. 2013;13(12):7814–7819. https://doi.org/10.1166/jnn.2013.8120
33. Iwashita T, Ando S. Preparation and characterization of ZnS thin films by the chemical bath deposition method. *Thin Solid Films*. 2012;520(24):7076–7082. https://doi.org/10.1016/j.tsf.2012.07.129
34. Mane RS, Lokhande CD. Chemical deposition method for metal chalcogenide thin films. *Mater Chem Phys*. 2000;65(1):1–31. https://doi.org/10.1016/S0254-0584(00)00217-0
35. Torabinejad M, Hong CU, McDonald F, Ford TP. Physical and chemical properties of a new root-end filling material. *J Endod*. 1995;21(7):349–353. https://doi.org/10.1016/S0099-2399(06)80967-2
36. Tec-Yam S, Rojas J, Rejón V, Oliva AI. High-quality antireflective ZnS thin films prepared by chemical bath deposition. *Mater Chem Phys*. 2012;136(2-3):386–393. https://doi.org/10.1016/j.matchemphys.2012.06.063
37. Zhong ZY, Cho ES, Kwon SJ. Characterization of the ZnS thin film buffer layer for Cu(In,Ga)Se2 solar cells deposited by chemical bath deposition process with different solution concentrations. *Mater Chem Phys*. 2012;135(2-3):287–292. https://doi.org/10.1016/j.matchemphys.2012.03.090
38. Khatri RP, Patel AJ. Thickness-dependent studies of chemically grown transparent conducting Cu:ZnS thin films for optoelectronic applications. *Opt Mater*. 2021;120:e111469. https://doi.org/10.1016/j.optmat.2021.111469
39. Zein R, Alghoraibi I. Influence of bath temperature and deposition time on topographical and optical properties of nanoparticles ZnS thin films

synthesized by a chemical bath deposition method. *J Nanomater*. 2019;2019:e7541863. https://doi.org/10.1155/2019/7541863

40. Maria KH, Sultana P, Asfia MB. Chemical bath deposition of aluminum doped zinc sulfide thin films using a non-toxic complexing agent: effect of aluminum doping on optical and electrical properties. *AIP Adv*. 2020;10(6):e065315. https://doi.org/10.1063/5.0011191
41. Arif N, Fun CS. Impact on the development of ZnS nanoparticles thin film deposited by chemical bath deposition and spin coating. *Int J Adv Eng Nano Technol*. 2021;4(5):1–4. https://doi.org/10.35940/ijaent.D0459.024521
42. Qi L, Mao G, Ao J. Chemical bath-deposited ZnS thin films: preparation and characterization. *Appl Surf Sci*. 2008;254(18):5711–5714. https://doi.org/10.1016/j.apsusc.2008.03.059
43. Ubale AU, Kulkarni DK. Preparation and study of thickness-dependent electrical characteristics of zinc sulfide thin films. *Bull Mater Sci*. 2005;28(1):43–47. http://doi.org/10.1007/BF02711171
44. Rathore KS, Patidar D, Janu Y, Saxena NS, Sharma K, Sharma TP. Structural and optical characterization of chemically synthesized ZnS nanoparticles. *Chalcogen Lett*. 2008;5(6):105–110. http://doi.org/10.13005/ojc/290341
45. Goudarzi A, Langroodi SM, Arefkhani M, Langeroodi NS. Study of optical properties of ZnS and MnZnS (ZnS/MnS) nanostructure thin films; Prepared by microwave-assisted chemical bath deposition method. *Mater Chem Phys*. 2022;275:e125103. https://doi.org/10.1016/j.matchemphys.2021.125103
46. Kumari P, Sharma A, Kumawat A, et al. Strong UV emission in flakes-like ZnS nanoparticles synthesized by cost-effective sol-gel method. *Mater Today: Proc*. 2022;58:642–647. https://doi.org/10.1016/j.matpr.2022.01.353
47. Jegalakshmi E, Rameshbabu M, Razia M, et al. Structural, optical, and antimicrobial activity of Ferric doped zinc sulfide (ZnS) nanoparticles. *Mater Today: Proc*. 2022;49:2611–2614. https://doi.org/10.1016/j.matpr.2021.07.274